

## Damage analysis of three-leg jacket platform due to ship collision

Jeremy Gunawan<sup>1</sup>, Jessica Rikanti Tawekal<sup>\*1,2</sup>,  
Ricky Lukman Tawekal<sup>1,2</sup> and Eko Charnius Ilman<sup>1,2</sup>

<sup>1</sup>Ocean Engineering Program, Institut Teknologi Bandung, Indonesia

<sup>2</sup>Offshore Engineering Research Group, Institut Teknologi Bandung, Indonesia

(Received October 19 2023, Revised November 25, 2023, Accepted December 12, 2023)

**Abstract.** A collision between a ship and an offshore platform may result in structural damage and closure; therefore, damage analysis is required to ensure the platform's integrity. This paper presents a damage assessment of a three-legged jacket platform subjected to ship collisions using the industrial finite element program Bentley SACS. This study considers two ships with displacements of 2,000 and 5,000 tons and forward speeds of 2 and 6.17 meters per second. Ship collision loads are applied as a simplified point load on the center of the platform's legs at inclinations of 1/7 and 1/8; diagonal bracing is also included. The jacket platform is modelled as beam elements, with the exception of the impacted jacket members, which are modelled as nonlinear shell elements with elasto-plastic material and constant isotropic hardening to provide realistic dented behavior due to ship collision load. The structural response is investigated, including kinetic energy transfer, stress distribution, and denting damage. The simulation results revealed that the difference in leg inclination has no effect on the level of localized denting damage. However, it was discovered that a leg with a greater inclination (1/8) resists structural displacement more effectively and absorbs less kinetic energy. In this instance, the three-legged platform collapses due to the absorption of 27.30 MJ of energy. These results provide crucial insights for enhancing offshore platform resilience and safety in high-traffic maritime regions, with implications for design and collision mitigation strategies.

**Keywords:** damage; displacement; failure; local denting; offshore platforms; ship collisions

### 1. Introduction

If a ship collides with an offshore platform, it can lead to structural issues. This is especially worrisome for platforms such as three-legged jacket platforms or those with fewer legs, as the failure of a single leg can jeopardize the structural integrity of the entire structure and disrupt production. According to Loughney *et al.* (2020), 176 ship collisions with offshore platforms have been reported. Numerous of these incidents rendered the platforms inoperable and caused operational losses.

Spouge (1999) defined ship collision criteria for platforms with four and eight legs. A collision with a four-legged jacket platform, for instance, causes the platform to collapse while absorbing 10 MJ of energy. This criterion is crucial for assessing the likelihood of failure in a timely manner (Tanujaya *et al.* 2022). Furnes and Amdahl (1980) evaluate the structural responses to a ship's side

---

\*Corresponding author, Dr., E-mail: jessicarikanti@itb.ac.id

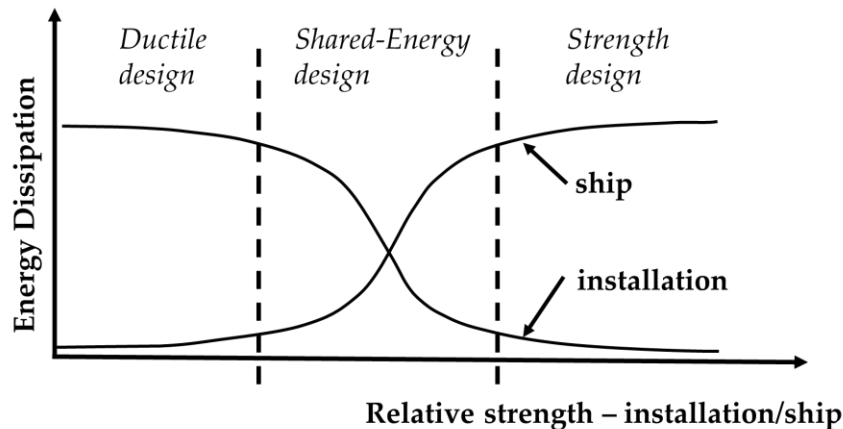


Fig. 1 Principal of Energy Dissipation

collision with a four-legged jacket platform and demonstrate that the platform absorbs the ship's kinetic energy via both local and global structural deformations, although the actual behavior is more complex (Amdahl and Eberg 1993). A subsequent study employs a complex finite element method to analyze the dynamic effects of a ship collision involving a four-legged jacket platform and a jack-up rig, assuming the impact load is a concentrated force. However, the existing literature contains few references to ship collisions involving platforms with only three legs.

When assessing platform-ship collisions, Sari *et al.* (2013) compared the results obtained using the simplified approach versus the finite element method in a separate study. The findings indicate that the simplified method yields results that closely resemble those of the more complex finite element modeling. This implies that the simplified method can effectively replace the complex nonlinear finite element analysis for offshore platform collisions, particularly for rapid assessment purposes.

When a platform collides with a ship, kinetic energy from the ship is converted into shared strain energy between the platform and the ship. The amount of energy that can be dissipated between a platform and a ship is determined by their respective stiffness levels. Fig. 1 (DNVGL, 2017) illustrates the relationship between energy dissipation and structural rigidity.

A robust design implies that the structure has sufficient strength to withstand excessive deformation, resulting in greater energy loss and ship deformation. In contrast, a structure or installation designed for ductility will absorb more energy than the vessel, resulting in greater structural deformation. Designing based on strength principles can result in higher expenses, whereas a ductility-oriented design will yield conservative outcomes. Storheim and Amdahl (2014) conducted a study on the design of offshore platforms to promote shared-energy designs, ensuring that collision energy is effectively dissipated between ships and structures.

The present study focuses on examining the damage characteristics resulting from a collision between a three-legged platform and a ship. It builds upon previous research into structural damages (Santoso *et al.* 2023, Tawekal *et al.* 2017, Tawekal and Iqbal 2008). This research contributes regarding energy absorption and structural responses in the context of a standard three-legged jacket platform, and serves as a fundamental reference for rapidly assessing the collision risk between offshore platforms and ships.

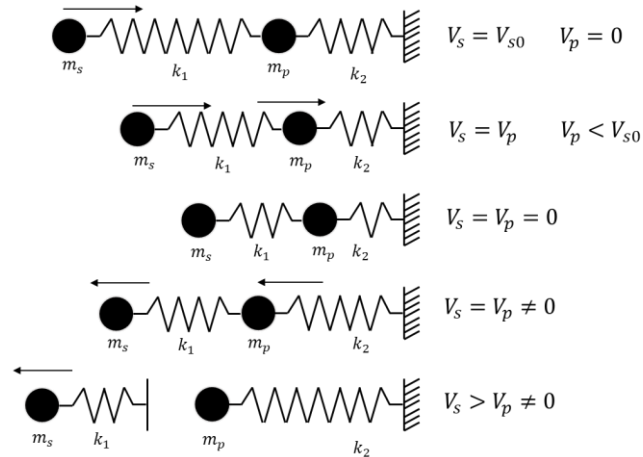


Fig. 2 Simplified Ship Collision Model (Sterndorff *et al.* 1992)

## 2. Methodology

### 2.1 General description

The primary purpose of the investigation is to evaluate the structural damage caused by ship collisions. The finite element method is used to simulate a three-legged platform. Fig. 2 presents a model that elucidates the collision dynamics of ships.  $m_p$  denotes the mass of the platform in this model, while  $m_s$  denotes the mass of the ship, including hydrodynamic added mass. The first phase entails the ship's motion and its impact on the installation. During this stage, a nonlinear spring denoted by the symbol  $k_1$  is introduced to represent deformation in both the ship and the structure. Kinetic energy is stored in the  $k_1$  and  $k_2$  springs, which represent the elastic energy of the structure.

Both the ship and the structure maintain identical speeds until the velocity reaches zero; this period corresponds to the moment of maximum contact force. When the spring  $k_2$  reaches its maximum state, it initiates the release of energy, which push the ship away from the structure. The unloading process persists during this phase until the ship and the structure are no longer in contact. Following the ship's separation from the structure, vibrations cause the structure to move independently.

In the model, beam elements are used to represent the jacket structure, with the exception of the impacted elements, which are represented by shell elements. The jacket platform's upper surface consists of three levels. As the ship geometry is not explicitly modelled, the collision force is applied as a concentrated load to a shell node. Fig. 3 depicts the relationship between load and deformation for the ship. This information, provided by Det Norske Veritas in 2017, is used to calculate the ship's stiffness for energy dissipation. The study assumes that the ship will collide with its bow.

### 2.2 Numerical model for platform-ship collision

Using the industrial finite element software Bentley SACS, which employs a dynamic response solver, a numerical model is constructed. With the exception of the impacted members, the entire

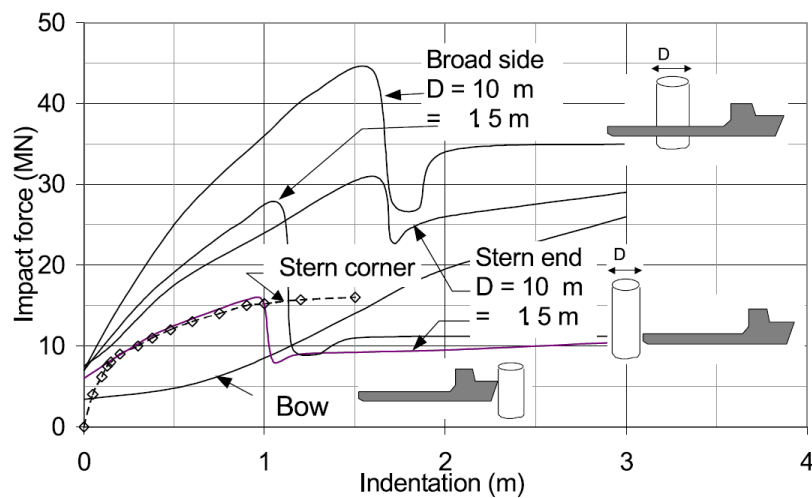


Fig. 3 Load Indentation Curve for Offshore Supply Vessels (DNVGL 2017)

three-legged jacket platform is represented by beam elements. The impacted legs have a circular cross-section with a diameter of 1100 mm and a thickness of 40 mm, whereas the impacted diagonal bracing has a circular cross-section with a diameter of 704.8 mm and a thickness of 28.58 mm. SACS's integrated shell-beam coupling is utilized to couple the shell's elements. The mesh size for beams is automatically determined by SACS, whereas the mesh size for shells is based on a mesh convergence study, as described in Section 2.4. The ship's collision contact with the affected member is defined as a simple point contact.

Forty mode shapes are extracted to generate modal solution and mass files. The dynamic response solver then uses these files to compute the structure's dynamic characteristics and loading effects. The collision load of the ship is represented as a point load on the impacted members. The analysis of ship impact includes a dynamic response analysis using the loads generated at each time step to determine the collapse response. The ship impact analysis continues until the impact joint's displacement exceeds the predetermined maximum deflection limit.

### 2.3 Material model

Table 1 details the yield strength of the jacket platform material used in this study. The density of steel is  $7850 \text{ kg/m}^3$ , the modulus of elasticity is 200 GPa, and the modulus is 80 GPa. To precisely analyze the denting and collapse behavior of members represented as shell elements, an elastoplastic material definition with constant isotropic hardening and a strain hardening ratio of 0.002 is used.

### 2.4 Mesh convergence study

To ensure convergence of the mesh, the shell elements within the impacted members in jacket leg are analyzed. Examining the von Mises stress at the collision contact node. The relationship between the number of elements and the stress at the node is depicted in Fig. 4. The results of the mesh convergence investigation indicate that the maximum shell mesh size of 1120 elements with a maximum mesh edge size of 119 mm is sufficient for the analysis.

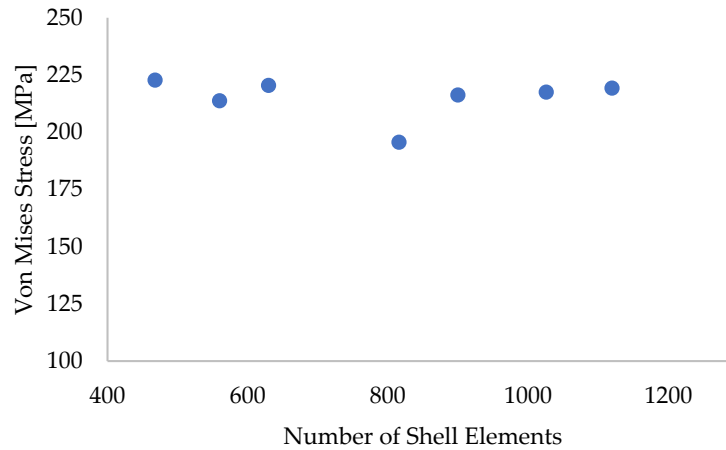


Fig. 4 Mesh Convergence for Shell Elements within the Jacket Leg

Table 1 Tubular Member *Dimensions and Yield Strength*

Member	Dimension (mm)	Yield Strength, $f_y$ (MPa)
Jacket Leg	Ø 1100 x 40	248
Joint Can	Ø 1100 x 48	345
Diagonal Brace	Ø 704.8 x 28.58	248
Pile	Ø 914 x 44.45	345

### 3. Case study

The three-legged jacket platform used in this study is derived from an existing platform design in the Makassar Strait region. As a result, the design has already satisfied the required criteria for in-place, seismic, and fatigue analyses, per API RP 2A (API, 2014). The collision location within jacket platform is defined by Norsok N-003 (Norsok 2017), which encompasses a vertical range between 10 meters below the lowest astronomical tide and 13 meters above the highest astronomical tide. As depicted in Fig. 5, the designated collision location ranges from -10.92 to +14.06 meters in height.

Two leg sections and one diagonal brace represent the portions of the model that will make contact with the ship. Shell elements are used to simulate these segments. The collision force of the vessel is applied as a concentrated load. According to Soreide and Amdahl (1983), head-on collisions generate a more concentrated force and more localized energy absorption than side impacts. Figs. 5 and 6 illustrates the positions of ship-platform contact nodes for different scenarios. It is assumed that the ship is moving towards the jacket legs for both 1/7 and 1/8 leg inclinations, as well as during interactions with the diagonal brace. The red arrows in Fig. 6 indicate the midspan collision contact nodes of the structural member. Table 1 provides structural member dimensions and yield strength.

Table 2 lists all the platform-ship collision cases utilized in this study. As stated by Spouge (1999), the displacement of supply vessels ranges from 2,000 to 5,000 tons. Different structural

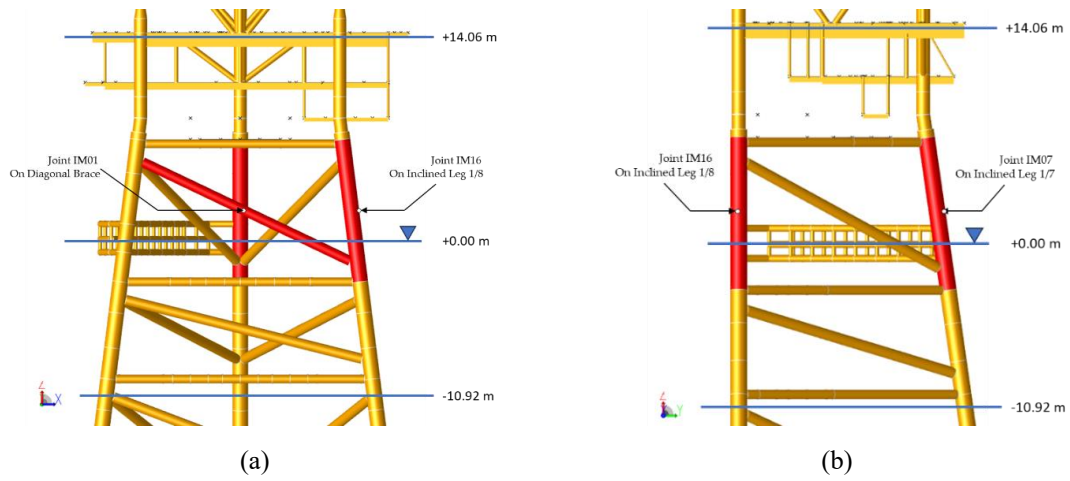


Fig. 3 Ship-Platform Contact Node Locations in Jacket Structure: (a) XZ Plan and (b) YZ Plan

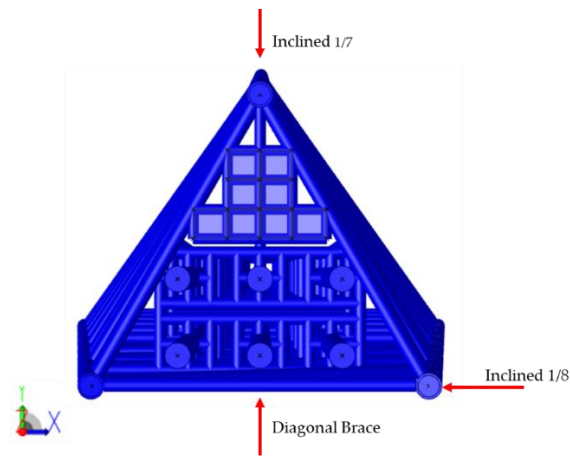


Fig. 4 Ship Direction to Jacket Platform.

Table 2 Ship-Platform Collision Cases

Case	Ship Displacement (tons)	Velocity (m/s)	Contact Node Location
M2V2DB	2,000	2	Diagonal Bracing
M5V2DB	5,000	2	Diagonal Bracing
M2V2I8	2,000	2	Inclined 1/8 Leg
M2V2I7	2,000	2	Inclined 1/7 Leg
M2V6I8	2,000	6.17	Inclined 1/8 Leg
M5V2I8	5,000	2	Inclined 1/8 Leg
M5V2I7	5,000	2	Inclined 1/7 Leg
M5V6I8	5,000	6.17	Inclined 1/8 Leg

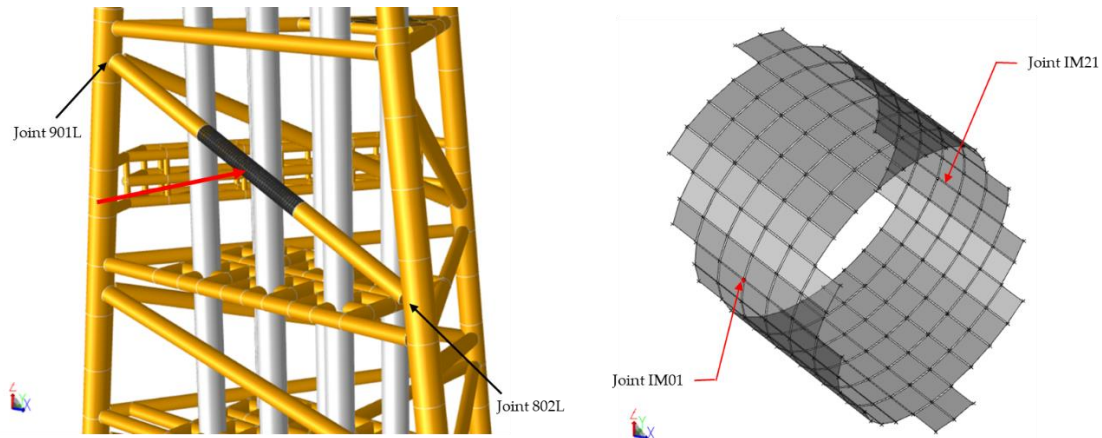


Fig. 5 Nodes Definition for Brace Impact Load Case (Case M2V2DB and M5V2DB).

reactions are produced by these vessel size. In this study, the smallest and largest vessel sizes are included in this study's case studies for ship-platform leg collisions. For passing vessels, Spouge advises an average speed of 12 knots, or 6.17 m/s. While for accidental limit state conditions API RP 2A WSD (API, 2014) recommends a ship velocity of 2 m/s. Different ship speeds will have different kinetic consequences.

## 4. Result and discussion

### 4.1 Collision of ship with platform's diagonal brace

As shown in Fig. 7, the portion of the diagonal brace of the jacket that was affected by the collision spans a distance of 16.70 meters, from Joint 901L to Joint 802L. However, only the 4-meter-long central segment of the diagonal brace is modelled using shell elements to reduce computational cost. These shell elements have an approximate edge size of 76 mm. The ship-platform contact node is specified as Joint IM01 at the midspan of the diagonal bracing. In contrast, Joint IM21 serves as a reference node for the non-dented part of the diagonal brace, which is located at the opposite side of the tubular member.

To minimize the impact on the jacket conductor, riser, or topside process equipment, it is essential to establish limitations on the extent of structural damage sustained by the affected structural member. According to DNVGL (2017), the prevention of damage to process equipment is contingent on limiting critical deflection. In this particular instance, a diagonal brace is located close to a conductor, highlighting the need to prevent excessive displacement. Fig. 8 depicts the distance between the diagonal brace and the conductor, which serves as an allowable criterion for diagonal brace displacement.

As shown in Fig. 9, the diagonal brace demonstrates deflection and contacts the central conductor. Due to no defined contact relationship between the diagonal brace and the conductor, the conductor's

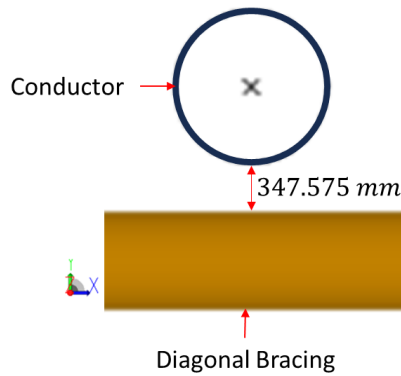


Fig. 6 Diagonal Brace Distance to Conductor

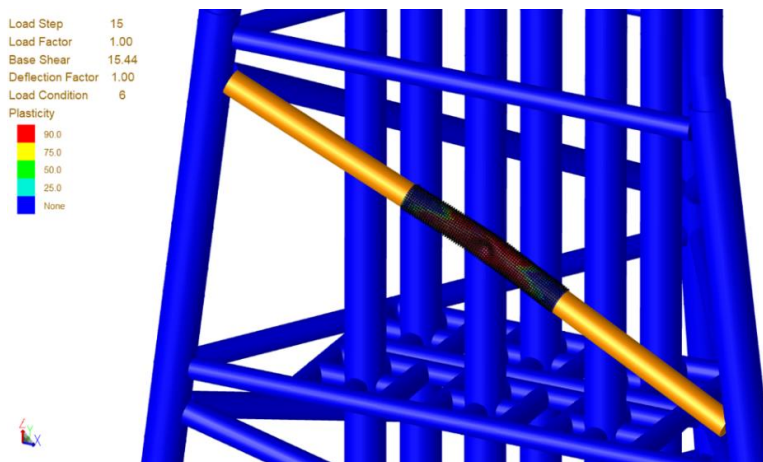


Fig. 7 Global Deflection of Diagonal Brace due to Ship Collision

response cannot be evaluated. Fig. 10 depicts the contact node forces and global displacements for different nodes, as depicted in Fig. 7.

The overall structural displacement at both extremities of the diagonal brace member, specifically Joint 901L and Joint 802L, was not significantly affected by the collision between the ship and the platform. The diagonal member exhibited a plastic bending deformation resistance, represented by the symbol  $R_0$  and calculated using the DNVGL (2017) formula, with a value of 1.69 MN. The contact node underwent deformation subsequent to the application of collision force, which led to the formation of a dent in the mid-section of the diagonal bracing. With an increase in the applied load, the diagonal brace member underwent deformation and established contact with the conductor at a contact node force of 3.014 MN, which exceeded the plastic bending resistance of the member. Variations in the ship's displacement had no discernible effect on the structural displacement and stress in this instance.

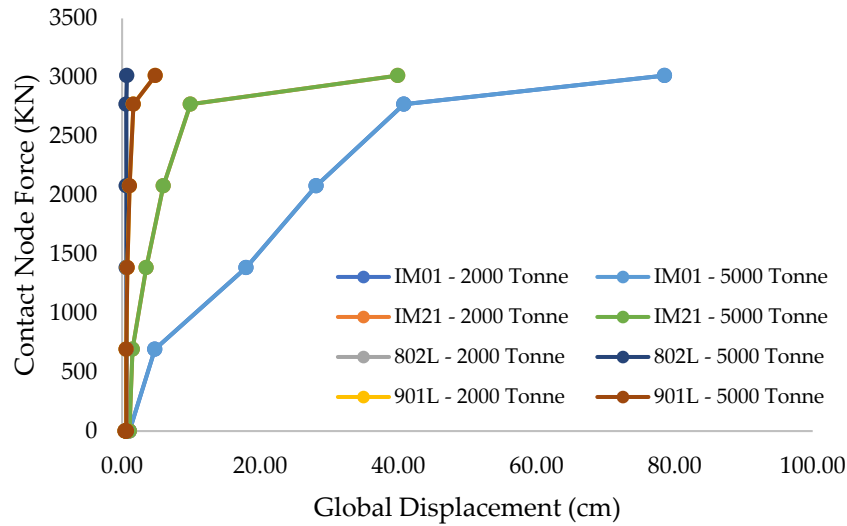


Fig. 8 Load Displacement Curve for Diagonal Brace Impact, Displaying Displacement in Several Nodes Defined in Fig. 7

Table 3 Energy Dissipation for Bow Against Brace Resistance (DNVGL, 2017)

Ship Contact Location	Energy Dissipation in Bow if Brace Resistance $R_0$			
	> 3 MN	> 6 MN	> 8 MN	> 10MN
Above Bulb	1 MJ	4 MJ	7 MJ	11 MJ
First Deck	0 MJ	2 MJ	4 MJ	17 MJ
First Deck – Oblique Brace	0 MJ	2 MJ	4 MJ	17 MJ
Between forecastle/First deck	1 MJ	5 MJ	10 MJ	15 MJ
Arbitrary Location	0 MJ	2 MJ	4 MJ	11 MJ

Table 3 delineates the energy dissipation that occurs in the bow of the vessel when it encounters the bracing, as reported by DNVGL (2017). The designed brace exhibits a comparatively moderate plastic bending resistance ( $R_0$ ) of 1.69 MN, which is lower than the minimum threshold of 3 MN necessary for the bow to efficiently dissipate energy. As a result, it is possible to deduce that the brace completely absorbs the kinetic energy. It is important to note, however, that Table 3 cannot be used to verify the dissipation of the ship's energy, as the ship is merely represented as a point load applied to the contact node. In accordance with the model proposed by Pacheco and Durkin in 1988, the idealized local denting consists of a flattened section and an undamaged section, as illustrated in Fig. 11. The assumption made in this particular instance of ideal local denting is that the member does not undergo any local bending as a result of the stress concentration, as described by Pacheco and Durkin (1988).

The force is distributed throughout the contact area that is created between the ship and the structure due to the deflection of the contact node. A visual representation of the depth of denting in the diagonal bracing is presented in Fig. 12. The depth of denting has been adjusted for normalisation

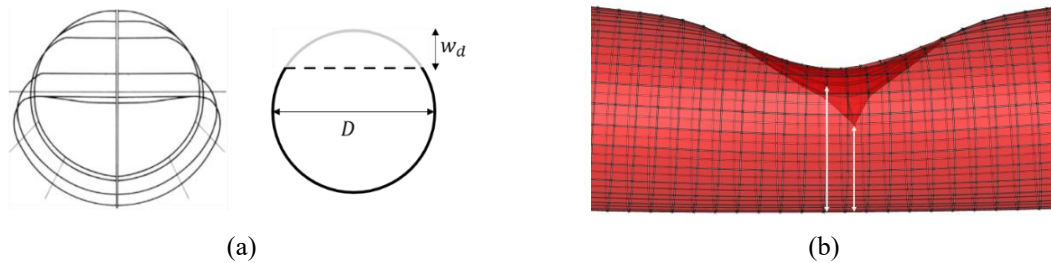


Fig. 9 Idealized Local Denting and Dent Depth for Brace Impact

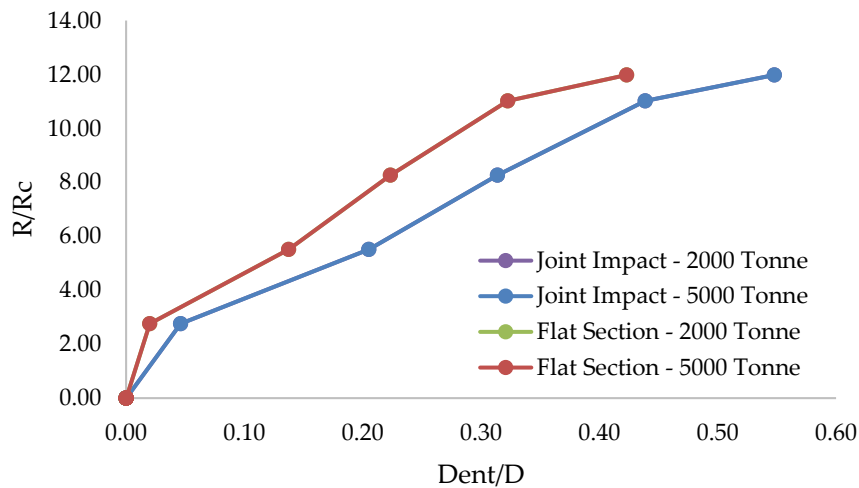


Fig. 10 Load-Indentation Curve for Diagonal Brace Impact

purposes in relation to the characteristic denting resistance,  $R_c$ , which was calculated using the DNVGL, 2017 method. In order to determine the depth of the dent, the relative depth of the flattened area is measured, as illustrated in Fig. 11(b), with the significant deformation at the contact node being disregarded.

#### 4.2 Collision of ship with platform's jacket leg

A segment of the jacket leg comprises several components, including a joint can, a jacket leg member, and a pile member. For the section of the jacket leg subjected to ship collision in this instance, it is represented using shell elements, with a maximum edge size of 119 mm, whereas the pile located within the jacket leg is modelled with shell elements with a maximum edge size of 99 mm. The leg and pile members are interconnected through a non-structural element referred to as a wishbone, which serves to transmit lateral loads from the leg to the pile. Three specific joints are considered for each leg: the contact node or joint IM16 on the leg with an inclination of 1/8, joint IM07 on the leg with an inclination of 1/7, joint 902L representing the end part of the leg member for inclination 1/8, joint 903L for inclination 1/7 representing the reference node of the leg member,

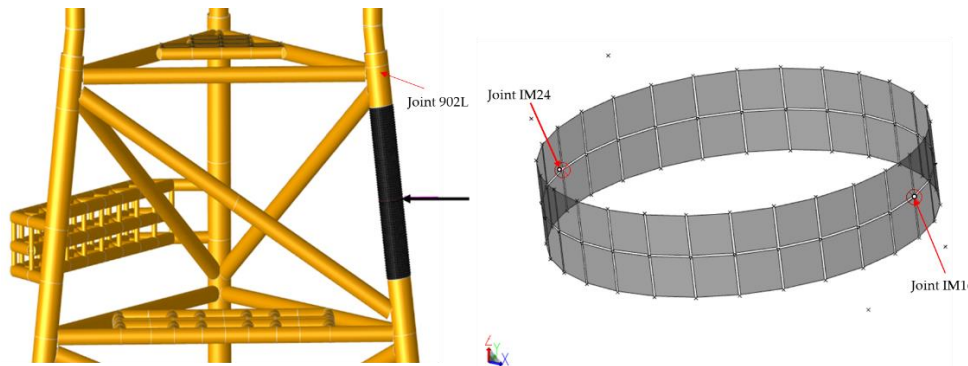


Fig. 11 Joint Definition for Impact Against Jacket Leg at 1/8 Leg Inclination

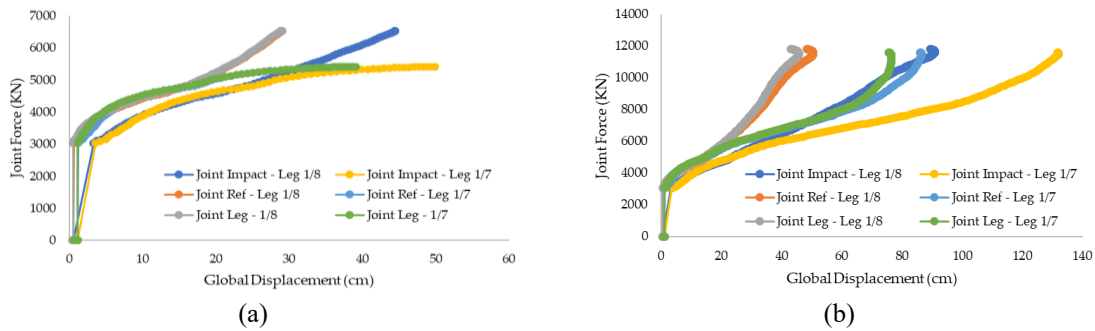


Fig. 12 Load Displacement Curve for Impact Against Jacket Leg for 2 m/s Ship Velocity using (a) 2,000 tons of ship's displacement and (b) 5,000 tons of ship's displacement

and node in joint IM24 for inclination 1/8, as well as joint IM20 for inclination 1/7, which represent the opposing part of contact node IM16. The positioning of the reference joints for leg inclination 1/8 is illustrated in Fig. 13.

In the context of collisions between a ship and a jacket leg, all such incidents are classified according to two distinct velocities: low-energy impacts pertain to incidents in which the vessel's velocity is 2 m/s or less, whereas high-energy impacts concern incidents in which the vessel velocity exceeds 12 knots or 6.17 m/s. When low-energy impact conditions are applied to a collision with a 2,000-ton vessel, the load-displacement patterns are depicted in Fig. 14. Without exceeding a certain threshold of collision force, it is indisputable that the contact node and the reference joints located at both extremities of the leg members, which symbolize the bending member, undergo consistent motion. The leg segment of the jacket is not susceptible to local bending in that member, as indicated by this observation. At the outset, the impact joint initiates its motion concurrent with the structure undergoing global deformation, which occurs as the contact node force increases. It indicates the presence of local deformation at the contact node if the displacement at that node exceeds that of the remaining reference nodes.

The differentiation is apparent in the load-displacement curve pertaining to low-energy impact collisions where supply vessels of 5,000 tons are involved. Initially, deformation is observed

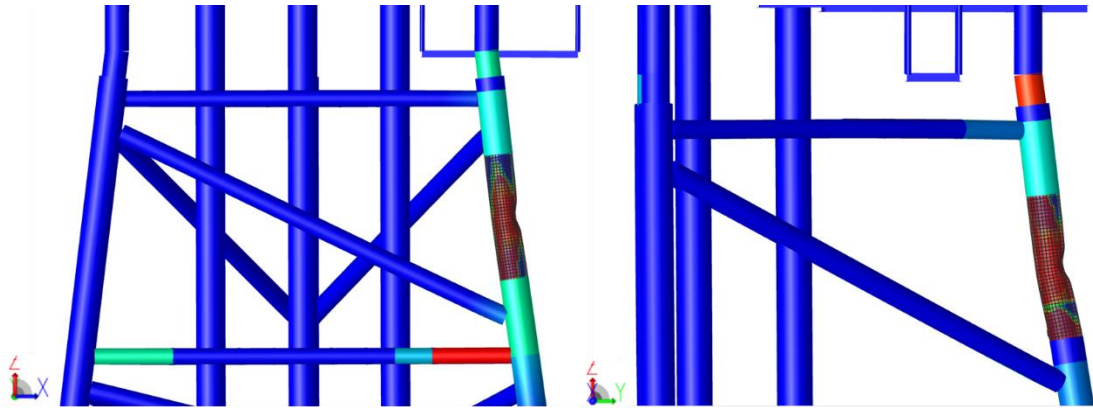


Fig. 13 Structure Global Deformation Case M5V218 and M5V217

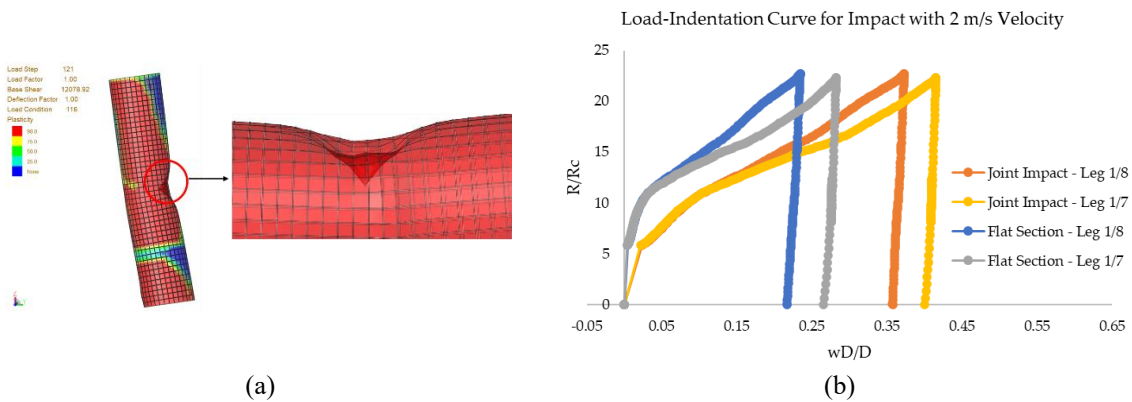


Fig. 14 Local Deformation for Ship Collision on Jacket Leg with 1/8 Inclination

between the contact node and the reference nodes when the vessel force is applied to the contact node, as illustrated in Fig. 14(b). An increase in the contact force results in a more pronounced deformation of the contact node in comparison to the other reference nodes; this indicates the presence of local deformation at the contact region. Both the member and the structure continue to deform until local bending becomes apparent at this stage. Jacket platforms that are exposed to a variety of low-energy impact vessels generally demonstrate comparable behavior. The structural deformation caused by a collision involving a 5,000-ton vessel displacement and a low-energy impact (Case M5V218 and M5V217) is depicted in Fig. 15. When a collision occurs, the primary member sustains the most severe structural damage.

The response of the localized deformation detected in the contact area during ship collisions differs significantly from collision scenarios in which diagonal bracing is utilized. Upon encountering a collision involving a vessel carrying a displacement of 2,000 tons, the dent penetrated to an estimated depth of 15% of the diameter. Furthermore, there was no indication of local bending in the jacket leg. This implies that the elastic phase accounted for the majority of energy dissipation in the structure, leading to worldwide displacement with only slight plastic deformation observed in

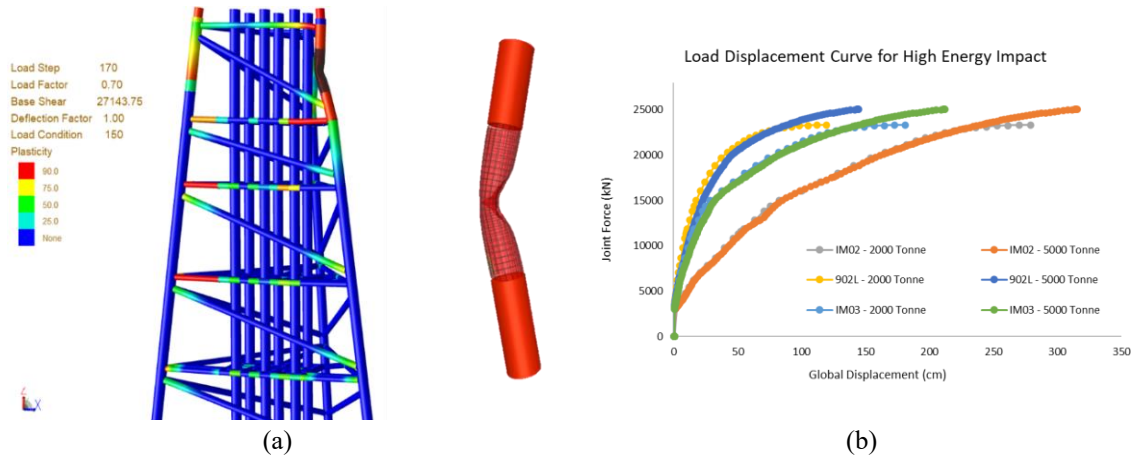


Fig. 15 Ship Impact Against Jacket Leg with Inclination of 1:8 using Ship Velocity 6.17 m/s

Table 4 Summary of Collision Result

Case	Maximum Contact Force (MN)	Maximum Displacement (cm)	Total Kinetic Energy (MJ)	Absorbed Energy by Structure (MJ)	% Absorbed Energy
M2V2I8	6.54	44.47	4.40	1.45	33.05
M2V6I8	23.00	279.15	38.07	16.60	43.61
M5V2I8	11.80	90.94	11.00	3.18	28.91
M5V6I8	25.00	315.34	104.70	27.30	24.63
M2V2I7	5.45	55.31	4.40	2.24	50.91
M5V2I7	11.60	132.09	11.00	3.73	33.91

the jacket leg. Visible damage commenced to result from collisions involving vessels of 5,000 tons. As illustrated in Fig. 13, collisions of low energy involving ships weighing 5,000 tons failed to cause significant damage to the structural members.

Fig. 16(a) illustrates a comparative analysis of local dent depths ( $wD/D$ ) as measured from the impact joint and the flattened area. Analogous to the effect observed on a diagonal brace, the application of a concentrated load results in a reduction in the depth of the depression, as depicted in Fig. 16(b). When implemented, the localized deformation in the vicinity and the contact area are both influenced by the inclination of the leg. In comparison to the leg with an inclination of 1/7, the leg with a 1/8 inclination undergoes a comparatively lesser amount of deformation. However, in evaluating the dent depth through the flattened section, the results are similar for both of these inclinations. Plastic deformation is the type of deformation that takes place within the collision zone, as indicated by the presence of unloading phases that ensue after the maximum force of the collision.

When the structure encounters a high-energy impact vessel, as observed in cases M2V6I8 and M5V6I8, the load-displacement curve for the reference nodes at the end of the leg is generated, as shown in Fig. 17(b) Significantly, during the initial phase, the displacement of the contact node is considerably more pronounced. Local deformation does not occur in the member during this initial

stage when the reference nodes of the end legs move in unison. The manifestation of local deformation occurs when the collision force attains 15 MN. In a similar fashion, the contact node experiences a significant displacement that coincides with the development of local denting.

Fig. 17(a) depicts the global deformation due to collision with vessel velocity of 6.17 m/s. jacket leg has undergone plastic deformation, and the jacket structure experience denting. Plasticity is also observed in several parts of jacket members.

A summary of all collisions between ships and platform jacket legs is provided in Table 4. In contrast to structures with equivalent total kinetic energy, instances characterized by greater contact forces exhibit a reduced capacity for energy absorption. This phenomenon arises due to the ship's internal energy absorption in addition to the kinetic energy dissipation transforming into integrated energy for the structure. This observation implies that the ship absorbs a greater quantity of energy as the collision force escalates.

The M5V6I8 structure assimilated 27.3 MJ of energy prior to undergoing a state of collapse subsequent to a high-energy impact. On the contrary, with regard to Spouge (1999), the ineffective jacket leg component withstood 10 MJ of energy. It is logical to hypothesize that the jacket leg itself absorbed 10 MJ; however, in this specific case, local denting occurred in both the leg and the pile contained within the jacket leg.

## 5. Conclusions

Various structural responses are apparent in the simulations of ship-platform collisions. Diagonal bracing does not exhibit a statistically significant effect on the overall structural performance when loaded, as opposed to situations in which inclined legs are loaded. Deformation of structural members ensues as the contact force increases, subsequent to their deformation. Notably, the impact of reduced kinetic energy on the local and global deformation of the contact nodes is negligible. A discernible increase in the local denting of the contact nodes is observed as the contact force escalates. Differences in the structure's inclination result in varying degrees of displacement and damage. Specifically, Jacket Legs inclined at a 1/7 angle experience greater displacement in comparison to those inclined at a 1/8 angle. It was ascertained, through the utilization of the stiffness characteristics of an offshore supply vessel illustrated in Fig. 3, that the energy absorption of the structure decreases with increasing contact force. When structural failure occurred, as in Case M5V6I8 involving a high kinetic energy, 27.30 MJ of energy was absorbed by the jacket platform.

## Acknowledgments

The authors gratefully acknowledge the financial support from Institut Teknologi Bandung for this work under research grants of Research, Community Service, and Innovation Program (P2MI).

## References

- Amdahl, J. and Eberg, E. (1993), Ship Collision with Offshore Structure. Structural Dynamics - EUROLYN.
- API, 2014. Recommended Practice for Planning, Designing and Constructing Fixed Offshore Platforms—Working Stress Design, 22nd Ed., API Publishing Service, Washington D.C.

- DNVGL (2017), Recommended Practice C204 - Design against accidental loads. DNVGL, Oslo.
- Furnes, O. and Amdahl, J. (1980), Ship Collision with Offshore Structure. Presented at the Proceedings of the Intermaritec '80, Hamburg.
- Loughney, S., Wang, J. and Wall, A. (2020), Ship/Platform Collision Incident Database (2015) for offshore oil and gas installations. <https://www.hse.gov.uk/research/rrhtm/rr1154.htm> (accessed 2.20.22).
- Norsok (2017), NORSOK N-003: 2017: Actions and actions effects. Norsok Lysaker, Norway.
- Pacheco, L.A. and Durkin, S. (1988), "Denting and collapse of tubular members—A numerical and experimental study", *Int. J. Mech. Sci.*, **30**, 317-331. [https://doi.org/10.1016/0020-7403\(88\)90104-X](https://doi.org/10.1016/0020-7403(88)90104-X).
- Santoso, J.F., Tawekal, R.L., Arianta, A. and Iلمان, E.C. (2023), "Numerical assesment of subsea pipeline capacity due to external circumferential semi-elliptical crack", *Int. J. Geomate*. **25**(8).
- Sari, A., Ghoneim, A. and Ayhan, Y. (2013), "Design and assessment of offshore structures for extreme and Abnormal Accidental Loading", Presented at the Offshore Technology Conference, OnePetro. <https://doi.org/10.4043/24084-MS>
- Spouge, J. (1999), A Guide to Quantitative Risk Assesment for Offshore Installations. CMPT.
- Sterndorff, M.J., Waegter, J. and Eilersen, C. (1992), "Design of fixed offshore platforms to dynamic ship impact loads", *J. Offshore Mech. Arct. Eng.*, **114**, 146-153. <https://doi.org/10.1115/1.2919966>.
- Storheim, M. and Amdahl, J. (2014), "Design of offshore structures against accidental ship collisions", *Mar. Struct.*, **37**, 135-172. <https://doi.org/10.1016/j.marstruc.2014.03.002>.
- Tanujaya, V.A., Tawekal, R.L. and Iلمان, E.C. (2022), "Vessel traffic geometric probability approaches with AIS data in active shipping lane for subsea pipeline quantitative risk assessment against third-party impact", *Ocean Syst. Eng.*, **12**(3), 267-284. <https://doi.org/10.12989/ose.2022.12.3.267>.
- Tawekal, R.L. and Iqbal, M. (2008), "Fatigue reliability index of jacket offshore platform based on fracture mechanics", *Proceedings of the EASEC-11 - Eleventh East Asia-Pacific Conference on Structural Engineering and Construction*.
- Tawekal, R.L., Prayudha, R. and Taufik, A. (2017), "Damage analysis of subsea pipeline due to anchor drag", **12**, 5016-5021.
- Tore S. and Jorgen, A. (1983), Energy absorption in ship-platform impacts. <https://doi.org/10.5169/seals-32418> (accessed 6.19.23).